LETTER **Communicated by James Reggia**

A Model of Indispensability of a Large Glial Layer in Cerebrovascular Circulation

Rohit Gandrakota
grohiit@gmail.com
V. S. Chakravarthy
schakra@ee.iitm.ac.in
Department of Biotechnology, Indian Institute of Technology, Madras, Chennai, 600036, India

Ranjan K. Pradhan
pkranjan@gmail.com
Biotechnology and Bioengineering Center, Medical College of Wisconsin, Wauwatosa, WI 53226, U.S.A.

We formulate the problem of oxygen delivery to neural tissue as a problem of association. Input to a pool of neurons in one brain area must be matched in space and time with metabolic inputs from the vascular network via the glial network. We thus have a model in which neural, glial, and vascular layers are connected bidirectionally, in that order. Connections between neuro-glial and glial-vascular stages are trained by an unsupervised learning mechanism such that input to the neural layer is sustained by the precisely patterned delivery of metabolic inputs from the vascular layer via the glial layer. Simulations show that the capacity of such a system to sustain patterns is weak when the glial layer is absent. Capacity is higher when a glial layer is present and increases with the layer size. The proposed formulation of neurovascular interactions raises many intriguing questions about the role of glial cells in cerebral circulation.

1 Introduction

Cerebral circulation involves interaction among the neural, glial, and vascular networks. The simplest form of blood flow regulation is by local regulation. Oxygen-deficient tissue releases vasodilators, which dilate local blood vessels, resulting in release of oxygen and nutrients. In the case of brain tissues, the metabolic needs are very high; though the brain is only 2% of the body weight, it uses 20% of cardiac output. Neural firing uses up the energy stored in ionic gradients across the membrane. The gradients are maintained by the action of ionic pumps, which depend on adenosine trisphosphate (ATP), produced by glucose and oxygen supplied by local blood flow.

Several signaling mechanisms are thought to underlie neurovascular coupling. For example, there is a direct mechanism by which neurons act on the vessels. Active neurons release glutamate, which opens N-methyl-D-aspartate (NMDA) receptors on other neurons, allowing the influx of Ca^{2+} ions into those neurons. Calcium activates nitric oxide-synthase (NO-synthase), which produces nitric oxide (NO), a potent vasodilator. Neurovascular signals are mediated by astrocytes also. Glutamate also binds to metabotropic glutamate receptors on astrocytes. This allows Ca^{2+} influx into astrocytes, which activates phospholipase A2 (PLA2) producing arachidonic acid (AA). Arachidonic acid (AA) is converted by cyclo-oxygenase into prostaglandin E2 (PGE2), a vasodilator released through the astrocytic endfeet contacting vessels (Haydon & Carmignoto, 2006).

Calcium signaling seems to play a key part in the mediating role of astrocytes in neurovascular coupling (Fellin & Carmignoto, 2004). Low-intensity neural activity produces a local increase of intracellular calcium ($[Ca^{2+}]_i$) typically confined to astrocyte processes, while stronger activity results in a widespread increase that spreads to neighboring astrocytes via gap junctions. Raised $[Ca^{2+}]_i$ can also spread to astrocyte end-feet surrounding vessel walls, resulting in the release of PGE2. Subsequently, PGE2 can cause vasodilation by directly acting on vascular smooth muscle or indirectly by acting on endothelial cells, which in turn mediate vasodilation (Fellin & Carmignoto, 2004). Thus we observe a spatially distributed signal that arises from a pool of neurons and, passing via a pool of astrocytes, acts on a mesh of microvessels.

What was described above was the signal that carries metabolic demands of neurons to the vascular network. There is also a reverse signal consisting of the flux of energy molecules like glucose and lactate from the vessels to neurons via astrocytes. In this reverse signaling too, astrocytes are thought to play a crucial role. A key event in this neurometabolic coupling is that glutamate stimulates aerobic glycolysis in astrocytes. Sodium-coupled reuptake of glutamate by astrocytes and the concomitant activation of Na-K-ATPase triggers glucose uptake and its glycolysis, which causes release of lactate from astrocytes. Lactate is thought to be the fuel for the energy demands associated with neural firing and synaptic transmission. Thus, glucose released by the vessels is picked by the glucose transporters in astrocytes and converted to lactate within astrocytes; lactate is then released to the neurons. Such a theory of neurometabolic processing, termed the astrocyte-neuron lactate shuttle (Pellerin et al., 1998), is supported by several lines of experimental investigation (Kasischke, Vishwasrao, Fisher, Zipfel, & Webb, 2004).

Computational modeling of neurovascular coupling is often motivated by the need to understand hemodynamic response, which forms the basis of most functional imaging techniques (Gibson, Farnell, & Bennett, 2007). Another motivation is to gain insight into disorders related to neurovascular phenomena like spreading depression (Kager, Wadman, & Somjen,

2000), cerebral ischemia (Revett, Ruppin, Goodall, & Reggia, 1998), migraine headache (Reggia & Montgomery, 1996), and stroke (Goodall, Reggia, Chen, Ruppin, & Whitney, 1997). Gibson et al. (2007) present a model that describes the chain of events from increased neural activity to local changes in CBF; astrocytes play a crucial role in this model. In the cerebrovascular network model of Boas, Jones, Devor, Huppert, and Dale (2008), the relation between cerebral metabolic rate and local changes CBF is expressed. However, the model has no explicit representation of neural or glial cells.

There are also models of neuro-glial interactions with no reference to vascular coupling. Nadkarni and Jung (2003, 2004) describe a model of activation of an astrocyte by a neuron via inositol 1,4,5-trisphosphate (IP3) production, which triggers the calcium release from the endoplasmic reticulum (ER). Increased Ca^{2+} levels in astrocyte activate the same neuron. This bidirectional interaction can cause oscillations that have been linked to epileptic seizures. Postnov, Ryazanova, and Sosnovtseva (2007) present a model of a tripartite synapse consisting of a presynaptic neuron, a postsynaptic neuron, the synapse connecting the two, and a glial cell (astrocyte). The model depicts the role of glial activity in long-term synaptic potentiation. Another model of the tripartite synapse (Nadkarni, Jung, & Levine, 2008) describes how glia can control synaptic transmission probabilities through bidirectional neuron-glia interactions. Somjen, Kager, and Wadman (2008) describe neuron-glia interactions through the mediating role of extracellular dynamics of ionic species like Ca^{2+} and K^{+}.

In an earlier work, we modeled oxygenation of skeletal muscle as an interaction between two networks: the network of motor neurons innervating muscle fibers and the vascular network (Pradhan & Chakravarthy, 2009). The model suggests that desynchronized dynamics of vessels ("vasomotion") and desynchronized activity of motor neurons enhance efficiency in oxygenation. The work presented here is an extension of the previous work on cerebral circulation, which involves three interacting networks: neural, glial, and vascular networks.

An investigation of local regulation of blood flow, particularly taken up in the context of cerebral circulation, raises an interesting question regarding the possible role of the glial network in neurovascular coupling. In most nonneural tissues, the tissue directly interacts with the vascular network by release of vasoactive substances. In neural tissue, however, this interaction takes place via an intermediate network: the glial network. The crucial role astrocytes play in forward and reverse signaling involved in neurovascular interactions is becoming increasingly clear. Why does the neural tissue require an intermediate network—a particularly large network, compared to the size of neural network—of glial cells to talk to the cerebrovascular system? To address this question through a simplified network model of neural-glial-vascular system is the objective of this letter.

We model cerebrovascular circulation as a network comprising three layers of oscillatory units: the neural, glial, and vascular layers. The proposed

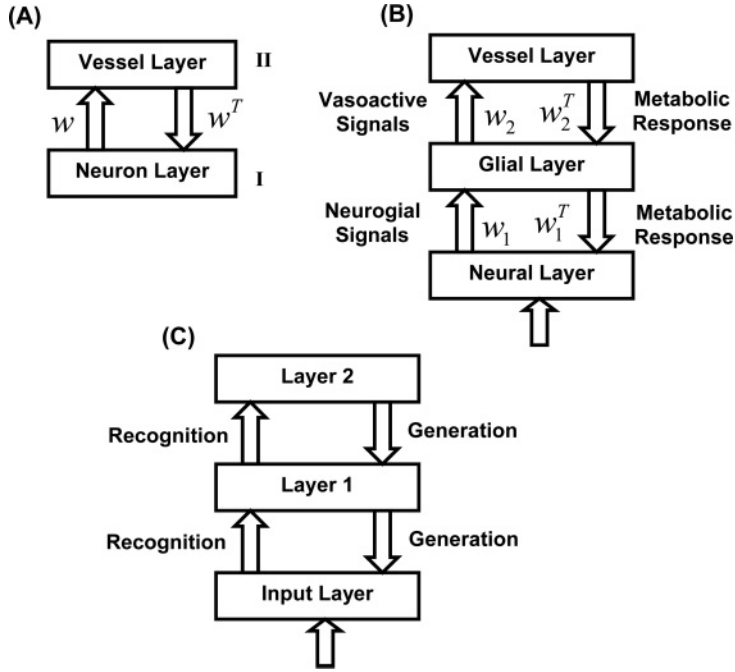

Figure 1: Configuration of a two-layer neuro-vascular network and a three-layer neuro-glial-vascular networks used in the model. (A) A two-layer neuro-vascular network consists of a neuron layer (layer I) and a vessel layer (layer II) with symmetrical bidirectional connections (w and w^T) between the layers. Each layer consists of ($m \times m$) units (neurons or vessels). (B) A neuro-glial-vascular network consists of three layers: neurons (layer I), glial cells (layer II), and vessels (layer III). Neural and vascular layers consist of ($m \times m$) units, while the glial layer consists of $n \times n$ units (neurons or glial cells or vessels). $w_1(w_1^T)$ and $w_2(w_2^T)$ are symmetrical weight matrices between the neuro-glial layer and glial-vessel layer, respectively. (C) A schematic of the deep belief network (adapted from (Hinton et al., 2006)) provided for comparison with the neuro-glial-vascular network of *B*.

model is a rather abstract one and is not meant to be a detailed biophysical model of the neuro-glial-vascular system. The network is designed such that input to a neural layer (assumed to arise from other neurons in the brain) is sustained by metabolic responses (we call them "nurturing echoes") from the vascular layer via the glial layer. Thus, network operation may be described as autoassociation, since an external input is sustained by a matching metabolic feedback. We use an unsupervised learning method similar to that used in deep belief networks of Hinton, Osindero, and Teh (2006). A schematic comparing the neuro-glial-vascular network with deep belief network is shown in Figure 1. The network is trained to sustain images of

handwritten digits from the MNIST database. Our model simulations show that the system fails to sustain more than a single pattern when only two layers (neural and vascular layers) are present; capacity to sustain more patterns increased when the intermediate glial layer is added.

The outline of the letter is as follows. Section 2 describes the model, and section 3 presents the results. Implications of the proposed perspective of neurovascular interaction are discussed in the final section.

2 Methods

2.1 Model Formulation. We study two different models consisting of two layers (neural-vascular) (see Figure 1A) and three layers (neural-glial-vascular), respectively (see Figure 1B). Each layer consists of oscillatory units connected laterally. Bidirectional connections are allowed between neural and vascular (w) layers in the two-layer model and neuro-glial (w_1) and glial-vascular (w_2) layers (in the three-layer model). Each layer consists of a two-dimensional square grid of nonlinear oscillators. Neural and vascular layers are fixed at a grid size of $m \times m$ each; however, the size of the glial layer, $n \times n$, is a variable. Learning consists of altering the neuro-glial and glio-vascular weights of the network.

All three layers consist of nonlinear oscillators with identical dynamics. The dynamics of a network or layer (neural or glial or vascular) of such units is written as

$$\frac{dx_i}{dt} = -x_i + \sum_{j=1}^{N} T_{ij} v_j - y_i + I_i \tag{2.1}$$

$$\frac{dy_i}{dt} = -y_i + v_i \tag{2.2}$$

$$v_i = \tanh(\lambda x_i), \tag{2.3}$$

where v_i is the state of the ith unit, x_i and y_i are internal variables, and I_i represents external input coming into the ith unit from another layer. A single unit in the above system can be shown to exhibit limit cycle oscillations for a certain range of inputs I (see Figure 3; for proof, see Gangadhar, Joseph, & Chakravarthy, 2007). T_{ij} represents the strength of lateral interaction between the ith and the jth unit in each layer. Since there are three layers (neural, glial, and vascular), there are, correspondingly, three sets of states, v_i^{neu}, v_i^{gli}, and v_i^{vas}, respectively, which biologically have different meanings in different layers. In the neural case, v_i^{neu} represents the firing rate of the neurons; in the glial case, v_i^{gli} is the cytosolic calcium concentration ($[Ca^{++}]_i$), which is the best indicator of glial activation; and in the vascular case, v_i^{vas} represents the size of the vessel lumen ($v_i^{vas} = 1$ denotes an open vessel; $= -1$ a closed vessel).

The motivation behind using oscillatory dynamics to describe the dynamics of neural, glial, and vascular units is as follows. Use of oscillatory dynamics to describe neural dynamics is not new and does not require special explanation. In fact, the proposed equations for a single unit are analogous to the two-variable FitzHugh-Nagumo model. Both models are capable of limit cycle (oscillations) and fixed-point dynamics. Glial cells do produce spontaneous oscillations, though for a long time, it was thought glial cells were under the passive control of neurons (Rose & Konnerth, 2001). Similarly, for a long time, it was thought that vessel activity is under the passive control of the neighboring tissue ("local regulation"), but later it was discovered that vessels have spontaneous oscillations—a phenomenon known as vasomotion (Nilsson & Aalkjaer, 2003).

The dynamics of the three layers are the same; therefore equations 2.1 to 2.3 are not repeated thrice for brevity of presentation. The distribution of the lateral weights in a layer is as follows:

$$\begin{aligned} T_{ij} &= \varepsilon - a \exp\left(-\frac{r_{ij}^2}{\sigma^2}\right), \quad for\ r_{ij} < R \\ &= 0, \qquad\qquad\qquad\qquad otherwise \end{aligned} \tag{2.4}$$

where r_{ij} is the Euclidean distance between the ith and the jth units, with coordinates $i = (i_{row},\ i_{col})$ and $j = (j_{row},\ j_{col})$, respectively, on the 2D layer. Thus, r_{ij} is the Euclidean distance between indices i and j. ε is a positive number between 0 and a, which controls the composition of positive and negative lateral connections among the units. R defines the radius of the neighborhood. Note that for $\varepsilon < 0$, lateral interaction among all the units in a layer is inhibitory; for $\varepsilon > a$, all the lateral connections are positive; for $0 \leq \varepsilon \leq$ a, lateral connections have a mix of excitatory and inhibitory connections, where the interaction with nearby neighbors is inhibitory and with distant neighbors it is excitatory (see Figure 2). Since there are three layers, there are actually three sets of lateral connections, T_{ij}^{neu}, T_{ij}^{gli}, and T_{ij}^{vas}, representing the neural, glial, and, vascular layers respectively. Since the dynamics are the same for the three layers, this notation is not reflected in equations 2.1 to 2.4. The sole purpose of the lateral inhibition-excitation model used is to define a mechanism by which activity within a layer can be synchronized or desynchronized by controlling the excitatory or inhibitory components of lateral connections. We have previously used the neighborhood function in this model in a different context to produce synchronization and desynchronization by varying a single parameter (Gangadhar, Joseph, & Chakravarthy, 2008). In this letter, however, we consider only desynchronized activity and set $\varepsilon = 0$ for all three layers.

The lateral weights too have biologically different meanings in different layers. In the neural layer, they obviously represent the synaptic strengths between neurons. In the case of glial cells, the lateral interactions

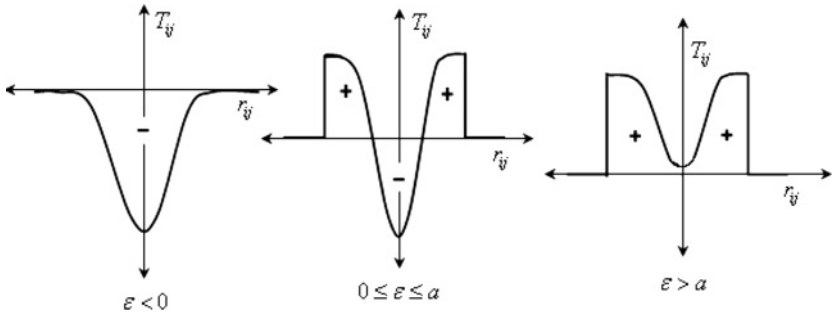

Figure 2: A diagrammatic representation of lateral weight distribution for different values of ε ($0 < \varepsilon < a$) and a fixed radius of neighborhood (R). The parameter ε controls the distribution of inhibitory ($-$ve sign) and excitatory ($+$ve sign) connections in each layer (neural, glial, and vascular layer). T_{ij} is the strength of the lateral connection for each layer (here T_{ij} represents T_{ij}^{neu}, T_{ij}^{gli}, and T_{ij}^{vas}); r_{ij} is the lateral distance between the ith and jth units in each layer.

represent the interglial interactions via gap junctions. Lateral interactions within the vascular layer require special mention. The microvascular network is usually thought to be a passive irrigation network supplying energy-rich molecules to metabolizing tissue. However, it can also be thought of as an informational network since information is exchanged among various parts of the network via a variety of signaling mechanisms (Secomb & Pries, 2002). Inspired by such a view of the microvascular system, we recently modeled vascular dynamics in skeletal muscle using a network of oscillators (Pradhan & Chakravarthy, 2009). Interactions among these vascular oscillators represent interactions among vessels by exchange of vascoactive substances. We adopt a similar model of vascular dynamics in the model examined here.

2.2 The Training Procedure. Training involves the adjustment of weights between the different layers: the neuro-vascular (w) stage in the first model and the neuro-glial (w_1) and glial-vascular (w_2) stages in the second model. The lateral connections T_{ij}^{neu}, T_{ij}^{gli}, and T_{ij}^{vas} are not trained. Fully connected weights between neighboring layers are assumed. Although there have been attempts to model a neuron-glia-vessel system as a chain of three single units (Gibson et al., 2007), a network structure with multiple units of each kind is more realistic. For example, each neuron interacts with many glial cells and vice versa. Similarly, each glial cell has its end-feet on multiple vessel segments. Thus, a fully connected network or a locally connected network is a more feasible option. But the choice between a fully connected network and a local network depends on the spatial scale at which the analysis is conducted. A fully connected network is meaningful if we consider

small tissue volumes, say, of the order of 10^6 cubic microns, which is what our model is proposed to represent.

The biological significance of connections between adjacent layers is now described. One mechanism of a glial (astrocytic) response to neural signals is described in the context of glutamatergic synapses. Glutamate release from a neuron binds to metabotropic receptors on the astrocytes, initiating a G-protein cascade that triggers the release of Ca^{2+} from internal stores "activating" the glia (Gibson et al., 2007). Thus, the forward connections from neuron to glial layer in the proposed model represent this strength of interaction between neurons and glia. The mechanism of vascular activation by release of vasoactive molecules by glia is more involved. ATP release from activated glia causes the release of nitric oxide (NO) from endothelial cells. NO acts on vascular smooth muscle, resulting in vasodilation (Gibson et al., 2007). Thus, the forward weights from glia to vessels represent, in an abstract way, the effect of glial activation on vascular lumen size. Dilated vessels release glucose, which is picked up by glucose transporters on glial cells. Thus, the relation between vessel lumen and glucose flux into glia is represented by the reverse connections from vascular to glial layer in the model. Glucose is converted to lactate within glia (astrocytes) and passed on to neurons (Pellerin et al., 1998). Lactate flux into neurons is denoted by the strength of reverse connections between the glial and neural layers.

The learning algorithm used in this model is based on a fast, greedy learning algorithm for multilayer networks suggested by Hinton et al. (2006). The inputs presented to the neural layer are 10×10 images of digits (0 to 9) from the MNIST database (size = 60,000 samples). In the bottom-up pass, interlayer weights are used to convert the input vector into a representation in the higher layers. Then, in the top-down pass, the interlayer weights are again used to reconstruct an approximation to the input vector from its underlying representation that is activated in the higher layer. The difference between the input vector and the reconstructed vector provides a measure of the network performance and reflects how well the weights are trained so as to enable the higher layers in storing the underlying representations of presented neural stimuli. If a vector p is presented to the network, that generates a response vector q in the next layer, the weight connecting the ith unit of the first layer and the jth unit of the second layer is updated as

$$\Delta w_{ij} = \eta(< p_i q_j >_{data} - < p_i q_j >_{recon}), \tag{2.5}$$

where η is the learning rate. Note that p and q correspond to states v's (see equation 2.3) of the units in a pair of adjacent layers in the model described in section 2.1. The state, q_i, of the ith unit in a given layer is a stochastic function of the state of the previous layer p and the interlayer connections, w_{ij}, as follows:

$$\Pr(q_i = 1) = \frac{1}{1 + \exp(-\sum_j w_{ij} p_j)}, \tag{2.6}$$

where $\Pr(q_i = 1)$ denotes the probability that q_i equals 1. The learning rate $\eta = 0.1$, as in the original Hinton model.

Training is performed one layer at a time. Once the weights between the neural and the glial layers are trained, the weights w_1 are frozen. The values of w_1 a fixed, and the weights w_2 are updated using the same learning algorithm (see equation 2.5). The responses of the glial layer units are treated as the data for the vascular layer. At any given layer, the input to that layer ("data") and the reconstruction by feedback from the next layer ("reconstruction") are used to train the weights between the two layers per equation 2.5. Once the w_2 weights are trained, they are fixed to again train the w_1 weights. This process is repeated over several passes.

2.3 Testing the Network. Testing the network simply means producing a response to an external input pattern and evaluating the error between the input pattern and the reconstruction. All the weights are frozen during this stage. The input pattern is presented as a constant input to the neural layer (as the external input I_i in equation 2.1). The response of the neural layer, v^{neu}, is passed through the neuro-glial connections (w_1) and presented to the glial layer as external input. Similarly, the response of the glial layer, v^{gli}, is passed through glial-vascular connections (w_2) and presented as external input to the vascular layer. This completes the forward pass. In the reverse pass, v^{vas}, is passed through vascular-glial connections (w_2^T) and presented as external input to glial layer; v^{gli} is passed through glial-neural connections (w_1^T) and given as external input to neural layer. This return signal from the glial to the neural layer is the "reconstruction." Note that during the testing phase, the stochastic state update, equation 2.6, is not used, and the desynchronized dynamics of equations 2.1 to 2.3 is used instead.

3 Results

The dynamic of a single nonlinear oscillator used for all three layers in the network is simulated. Figure 3A shows the variation of state (v) of a single oscillator with time (iteration). It is observed that for suitable parameter values ($I = (-0.2 \text{ to } 0.2)$, $\lambda = 3$) the system exhibits self-sustained oscillation (limit cycle), and a formal proof for existence of the limit cycle for $I = 0$ is given in Gangadhar et al. (2007).

A two-dimensional array of oscillators described above is now simulated for various values of ε. Array size $= 15 \times 15$; the parameters a and R in equation 2.4 are 2 and 3, respectively; ε is varied from 0 to a (=2) in steps of 0.4. The results are shown in Figure 4.

We now proceed to construct the neuro-vascular and neuro-glial-vascular networks. Training of these networks is performed using the deep belief algorithm (http://www.cs.toronto.edu/~hinton/MatlabForSciencePaper.html). Training the network with oscillatory layers

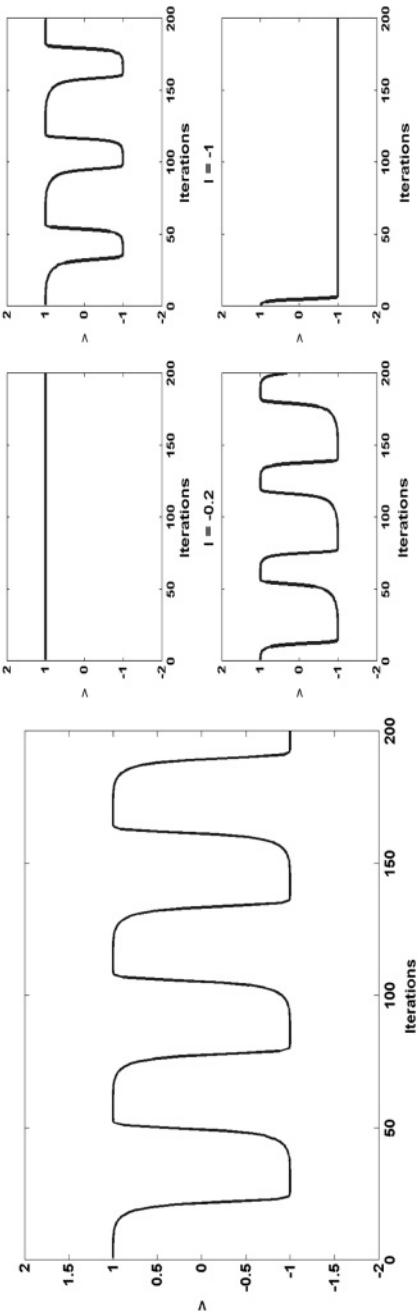

Figure 3: (A) The behavior of a single isolated oscillator used in the neuro-glia vessel network in the model for $I = 0$. (B) For $I > 0.27$, the output, v, of the unit saturates at $v = 1$; for $I < -0.27$, the unit saturates at $v = -1$.

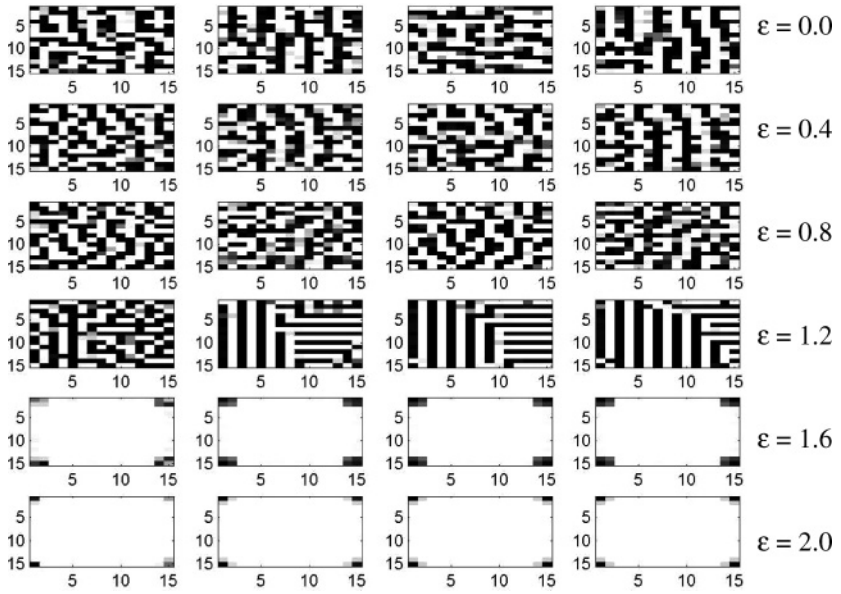

Figure 4: Results of simulation of an array (15 × 15) of oscillators described by equations 2.1 to 2.4. ε increases from 0 to 2 in steps of 0.4 from top row to bottom row. The columns represent the snapshots of the oscillator activity (v) at iteration numbers 20, 40, 60, and 80. Note that though the input patterns are binary, the state of the units is the output of a tanh(.) function and therefore take continuous values from -1 to 1. Hence the reconstructed image is a gray-scale image.

is found to be time-consuming, since oscillatory dynamics are computationally intensive. Note that the deep belief algorithm uses stochastic units. Therefore, we use layers containing stochastic units as in the original deep belief network while training; the stochastic layers are substituted by the oscillatory layers described above to simulate retrieval operations.

3.1 Simulation with the Neuro-Vascular Network. First, a two-layer network (only neural and vascular layers) with 10 × 10 units ($m = 10$) in each layer is simulated. The size of the weight matrix w is 100 × 100 ($m = 10$). Input is presented to the first layer as a 10 × 10 image, which is passed through the weights to produce the response of the vessel layer; w^T is used for the reconstruction of the input. The following parameter values are used in the lateral connections, for both neural and vascular layers: $\varepsilon = 0$ and $\sigma = 4,\ R = 12$. The two-layer network, on training with 60,000 examples of digits from 0 to 9, has given the results shown in Figure 5 on a test data set of 500 samples per class from digits 0 to 9. Figure 5 shows the reconstructed image of the network for sample inputs corresponding to three digits: 0, 1, and 2. Note that the performance of the two-layer

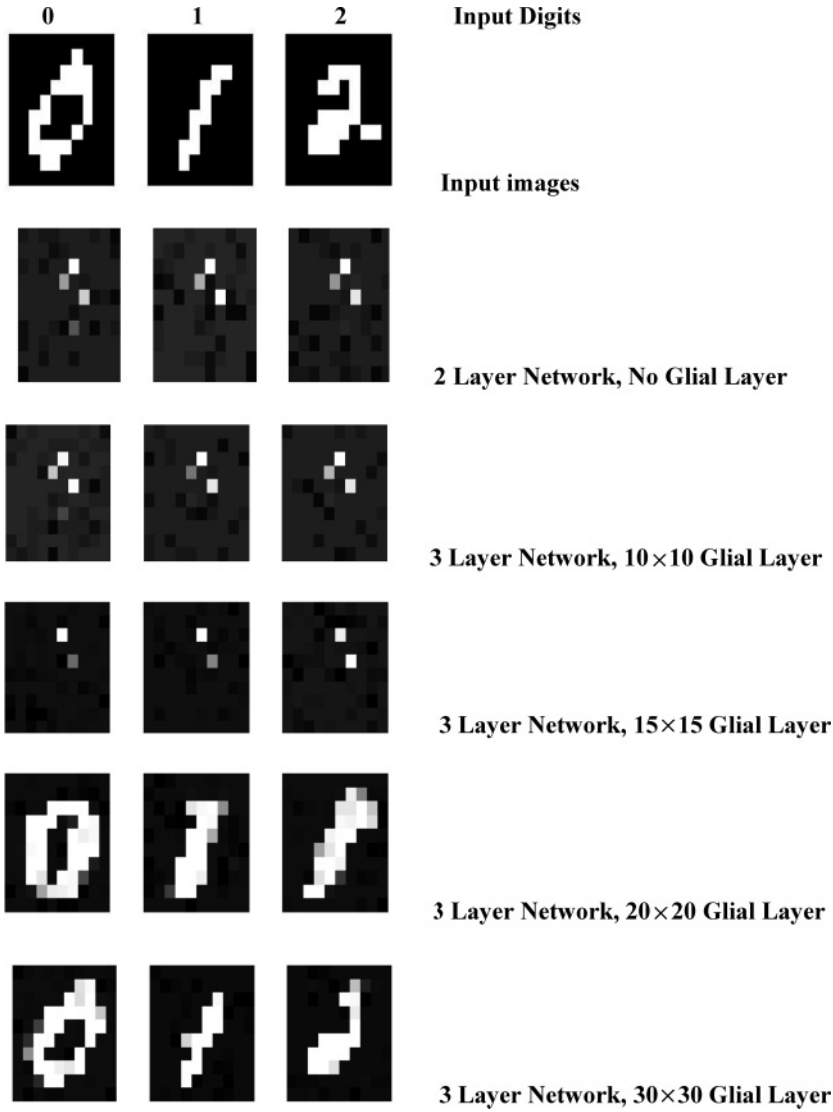

Figure 5: Reconstruction images of different types of networks for three arbitrarily chosen input digits. Shown here are the reconstruction of input digits 0, 1, and 2 using various network architectures. In the two-layer network (neuro-vascular), the size of the neural and vascular layer is set to 10×10 units. For all three layer networks (neuro, glia, vascular), the size of neural and vascular layers is set as 10×10 for simulation while the number of glial cells varies in each network (as shown in right panel). Same gray scale as in Figure 4.

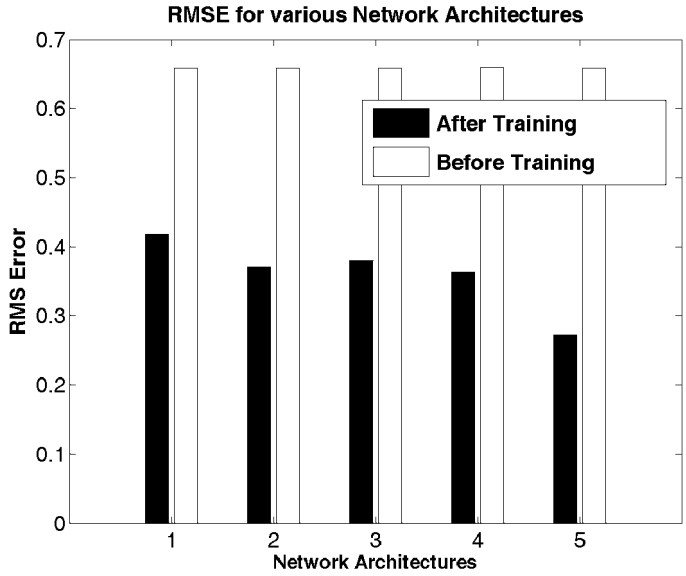

Figure 6: Reconstruction error (RMSE) results of various network architectures before and after training. RMSE before and after training for a (1) two-layer neurovascular network, (2) three-layer network with a glial layer of 10×10, (3) three-layer network with a glial layer of 15×15, (4) three-layer network with a glial layer of 20×20, and (5) three-layer network with a glial layer of 30×30.

network is unacceptable. Hence, a three-layer model is simulated to solve this problem.

3.2 Simulation with the Neuro-Glial-Vascular Network. For simulations and training of the neuro-glia-vascular network, we considered four cases based on the size of the intermediate glial layer (case 1: $m = 10,\ n = 10$; case 2: $m = 10,\ n = 15$; case 3: $m = 10,\ n = 20$; case 4: $m = 10,\ n = 30$), whereas the size of neuron and vessel layers in the network is held constant ($m \times m$). The following parameter values are used in the lateral connections: $\varepsilon = 0$ for all three layers and $\sigma = 4$ for both neural and vascular layers, and for the glial layer, $\sigma = 0.4\,n$, where $n \times n$ is the size of the glial layer. For all four cases, the network is trained with 60,000 examples of digits from 0 to 9 and tested on 5,000 digits from 0 to 9. The test data is nonoverlapping with the training data. Network reconstructions for sample inputs are shown for each of the four cases in Figure 5. Average performance, measured by root mean squared error (RMSE), over all digits is shown in Figure 6. Note that since the network layers are dynamic, the response of the neural, glial, and vascular layers varies with time even for a constant input. (A sample response of the network with a 20×20 glial layer is shown in Figure 7.)

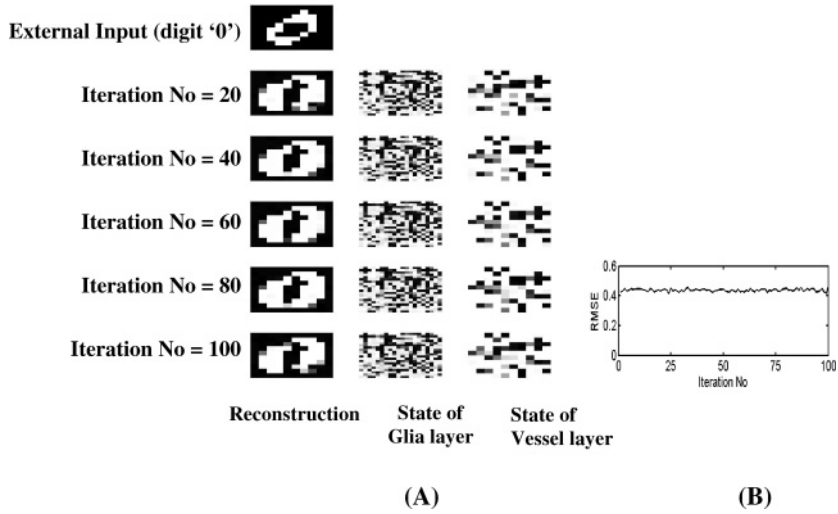

Figure 7: (A) The response of the network with a 20×20 glial layer ($n = 20$) to a constant external input (digit 0), which is shown as a single image in the top row. In every subsequent row, the image on the left is the reconstruction, the image in the center is the state of the glial layer, and the one on the right is the state of the vessel layer. Rows 2–6 correspond to iteration numbers 20, 40, 60, 80, 100. (B) RMSE of reconstruction shown as a function of time (iteration).

Thus, the network's performance summarized in Figure 6 is evaluated over reconstructed images averaged over 20 iterations and over 500 samples, plus all digit classes from 0 to 9. Note that reconstruction quality is poor for glial layer sizes of 10×10 and 15×15 (see Figure 5). The 20×20 glial layer size is considerably superior to that of the two previous cases, but important features of the input image (as in case of the digit 2) are omitted. The RMSE variation does not sensitively reflect the reconstruction performance because it is averaged over a large number of samples.

4 Discussion

The computational models for neurovascular coupling that were proposed earlier considered metabolic processes in neural networks (Gibson et al., 2007). But in those models, the neuronal networks are not engaged in any form of information processing or learning. The novelty in the model presented here is that the problem of cerebral circulation is formulated as a problem of association, and therefore unsupervised learning techniques are applied to design the neural-glial-vascular interactions. Such a perspective of neuro-glial-vascular interactions is quite radical and opens up a number of interesting questions. The neural layer receives inputs from an external

source. In order for this input to produce a stable response in the neural layer, the local metabolic demand generated by the neural layer must be sustained by a precisely patterned local metabolic supply from the vascular layer via the glial layer. We suggest that such a mechanism is similar to an associative network with unsupervised learning exemplified by the deep belief network of Hinton et al. (2006).

This letter asks an important question: Is the glial layer indispensable for neurovascular coupling? Does cerebral circulation offer special constraints, nonexistent in nonneural tissue, that require the agency of an intermediate network like the glial network? It may be expected that neural tissue, by its very nature, needs to support spatiotemporal activity patterns of far greater complexity than in other forms of tissue. Therefore, in order to achieve a precisely patterned delivery of oxygen and nutrients that match the metabolic demand of neurons, it might be necessary to have a large intermediate layer of cells, a function that is probably served by glial cells, particularly astrocytes.

Glial cells, particularly astrocytes, play a crucial role in the supply of energy to neurons by regulating the rate of glucose uptake and phosphorylation in response to glutamate concentrations in the synaptic cleft (Tsacopoulos & Magistretti, 1996). Thus, the local density of glial cells is an indicator of the metabolic demand of local neural tissue (Sherwood et al., 2006). Evidence exists that the glial-neuron ratio increases with higher environmental enrichment and stimulation (Diamond, Krech, & Rosenzweig, 1964; Szeligo & Leblond, 1977). Thus, the perspective of the glial layer role in neurovascular coupling embodied by the model presented here is in line with the known biology of neuro-glial tissue.

However, we do not claim that the model presented is a quantitatively accurate model of neuro-glial-vascular interactions. It is an abstract network model whose aim is to describe the neuro-glial-vascular interactions as being driven by associative, unsupervised learning mechanisms. Several simplifying assumptions have been made. All three kinds of cells—neurons, glia and vessels—are modeled by the same equations describing a nonlinear oscillator. Unlike the deep belief network, which uses stochastic units, we use a network of oscillators with mostly inhibitory lateral connections in order to produce desynchronized activity. Such desynchronized activity serves as a deterministic substitute to stochasticity in the original deep belief network model. In the two-layer model of section 3.1, it was possible to store only a single pattern. This is probably a peculiarity of our model, which need not be the case for general two-layer networks trained by associative learning. For example, in bidirectional associative memory with deterministic units, it was shown that a rough estimate of capacity is $\min(m, n)$, where m and n are sizes of the two layers (Kosko, 1992). In the case of the three-layer model of section 3.2, it was possible to store and retrieve all 10 patterns only when the glial layer was nine times larger than the neural layer. These glial-neuron ratios are not meant to correspond quantitatively

to the glial-neuron ratios observed in mammalian cortices. Another assumption made regarding the connections for mathematical convenience is the symmetry assumption, which must be relaxed in future developments of the model. Furthermore, neurons can directly act on vessels by release of NO, which implies the existence of direct neuron-vessel connections, which are omitted in the model (Lee, 2000).

There is another interesting question regarding the possible role of the (de)synchronized activity of neurons in cerebral circulation. Our earlier modeling work suggested that the desynchronized activity of motor neurons and vessels in skeletal muscle enhances efficiency in oxygenation (Pradhan & Chakravarthy, 2007, 2009; Pradhan, Chakravarthy, & Prabhakar, 2007). By increasing the composition of excitatory connections, it is possible to switch from desynchronized to synchronized activity. This is the intent behind using deterministic oscillator units with lateral connections instead of using stochastic units, as was done in deep belief networks (Hinton et al., 2006). It would be interesting to study an analogous role of desynchronized activity in neural, glial, or vascular dynamics in cerebral circulation. However, the role of desynchronized activity in cerebral circulation does not form part of this study.

The idea of applying learning techniques to explain neuro-glial-vascular interactions has interesting consequences. Neurons act on glial cells by the release of neurotransmitters; glial cells act on the vessels by the release of vasoactive substances. Is there evidence for activity-dependent adaptation similar to synapses in these various interactions? Activity-dependent neuronal-glial remodeling was discovered in the adult rat hypothalamus (Theodosis & Poulain, 1993). Astrocytes can encode different levels of neuronal activity into specific Ca^{2+} oscillation frequencies, which, at the level of perivascular end-feet, mediate the release of vasodilators such as 8,9-epoxyeicosatrienoic acid (EET), or vasoconstrictors such as monohydroxyeicosatetraenoic acids (20-HETE). Neuronal activity-dependent Ca^{2+}oscillations may ultimately represent the signaling system that allows blood flow to be proportional to the intensity of neuronal activity (Haydon & Carmignoto, 2006). In this letter, we suggest activity-dependent adaptation of the delivery of metabolites from the vessels via the glial network. Such a notion follows naturally if we accept the view that perfusion may be treated as a problem of autoassociation. In fact, there exists an interesting notion of metabolic plasticity, which envisages activity-dependent changes in metabolic patterns (Magistretti, 2006). Indeed, there also exists experimental evidence, albeit restricted, for activity-dependent long-term adaptation in such metabolic plasticity (Barrett, Shumake, Jones, & Gonzalez-Lima, 2003; Gonzalez-Lima & Garrosa, 1991; Zhang & Wong-Riley, 1999).

Traditionally glial cells have been thought to perform auxiliary support functions like calcium and potassium buffering and scavenging, for example. But glial signaling does not seem to be limited to rendering these services to neurons. The glial network is thought to play a crucial intermediary

role in transferring signals of metabolic demand from neurons to microvessels (Charles, 2005). In the reverse direction, the glial layer seems to play a key role in receiving energy molecules from the vascular layer, transforming and distributing them to the neural layer (Charles, 2005; Magistretti, 2006). Thus, far from being a passive support network, the glial layer seems to play a dual role—as a signaling network in the neuron-vessel direction and as a metabolic distribution network in the vessel-neuron direction—in coordinating the brain's energy exchanges.

Glial function is often described as if it is under the passive control of signals arising from the neural layer. However, low-frequency spontaneous Ca^{2+} oscillations have been discovered in glial cells. These oscillations are shown to cause NMDA-receptor-dependent excitation and calcium transients in neighboring neurons (Rose & Konnerth, 2001). Furthermore, calcium changes in astrocytes have also been shown to result in Ca^{2+} oscillations in myocytes of parenchymal arterioles in brain slices (Filosa, Boney, & Nelson, 2004). Thus, calcium oscillations seem to be the common currency through which the glial layer coordinates neurovascular coupling in the brain. However, analogous to the spontaneous glial Ca^{2+} oscillations, microvessels are also capable of spontaneous oscillations of lumen termed vasomotion (Nilsson & Aalkjaer, 2003). These mechanical oscillations of the vessel wall are associated with oscillations in membrane potential, which in turn is associated with intracellular Ca^{2+} oscillations of vascular smooth muscle. In the light of such experimental evidence, it is perhaps more appropriate to describe neural, glial, and vascular layers as three independent networks capable of spontaneous activity but working in tandem to perform metabolic functions of the brain. Therefore, a description in which glial and vascular layers are subservient to neural signals is perhaps not accurate. This relative independence of neural, glial, and vascular layers is reflected in the model presented here by the choice of three interacting layers, each capable of producing spontaneous oscillations.

Although Ca^{2+} oscillations are a common link among neural, glial, and vascular dynamics, the frequencies involved are not the same. The frequency of spontaneous glial Ca^{2+} oscillations is about 0.003 Hz (Rose & Konnerth, 2001; Parri, Gold, & Crunelli, 2001) and the frequency of associated vascular Ca^{2+} oscillations is about 0.18 Hz (Filosa et al., 2004). Transients in neuronal $[Ca^{2+}]_i$ correlated with astrocytic $[Ca^{2+}]_i$ are observed, though precise frequency information regarding neural $[Ca^{2+}]$ oscillations is not available. However, neuroglial interactions seem to be happening at a much slower timescale compared to the timescale of neural spiking. Thus, there are multiple timescales involved not only across layers, but also in individual layers, for example, signaling inside neurons involves both fast spiking and slow calcium oscillations. These differences in timescales involved in neuro-glio-vascular interactions are not captured in our model, which assumes oscillators of same frequency in all the three layers. A more detailed treatment of different timescales will be a part of the future work.

The traditional view of computation in the brain regards neurons as the primary agents of information processing. There is now enough evidence to show that astrocytes are also involved in information processing. A recent work goes as far as describing astrocytes of visual cortex as having "tuned responses" to visual stimuli (Schummers, Yu, & Sur, 2008). Our model extends this trend conceptually and proposes that the brain's computations are executed by the neuro-glial-vascular network. Is it conceivable then to talk of "tuned responses" in microvessels to sensory stimuli? Can one imagine an arteriole in visual cortex that preferentially dilates when a bar of a given orientation is presented in the receptive field of a neuron in the neighborhood?

A novel aspect of the proposed model is to place neural, glial, and vascular networks on a similar footing and treat them as networks working in tandem, with the intention of suggesting functional parallels between neural (and glial) and vascular networks. But structural parallels between the nervous system and cardiovascular system were observed hundreds of years ago, in 1543, by Belgian anatomist Vesalius. Blood vessels and nerve fibers course throughout the body in an orderly pattern, often alongside one another. The mechanisms involved in wiring neural and vascular networks share some deep similarities. Axons are guided to their targets by finely tuned codes of attractive and repulsive cues, and these cues also help blood vessels navigate to their targets (Carmeliet & Tessier-Lavigne, 2005). These data suggest that there might be deep functional similarities in the dynamics of neural and vascular networks, which is a strong underlying theme of this letter.

References

Barrett, D., Shumake, J., Jones, D., & Gonzalez-Lima, F. (2003). Metabolic mapping of mouse brain activity after extinction of a conditioned emotional response. *J. Neurosci., 23*, 5740–5749.

Boas, D. A., Jones, S. R., Devor, A., Huppert, T. J., & Dale, A. M. (2008). A vascular anatomical network model of the spatio-temporal response to brain activation. *Neuroimage, 40*, 1116–1129.

Carmeliet, P., & Tessier-Lavigne, M. (2005). Common mechanisms of nerve and blood vessel wiring. *Nature, 436*, 193–200.

Charles, A. (2005). Reaching out beyond the synapse: Glial intercellular waves coordinate metabolism. *Sci. STKE, 2005*, pe6.

Diamond, M. C., Krech, D., & Rosenzweig, M. R. (1964). The effects of an enriched environment on the histology of the rat cerebral cortex. *J. Comp. Neurol., 123*, 111–120.

Fellin, T., & Carmignoto, G. (2004). Neurone-to-astrocyte signalling in the brain represents a distinct multifunctional unit. *J. Physiol., 559*, 3–15.

Filosa, J. A., Boney, A. D., & Nelson, M. T. (2004). Calcium dynamics in cortical astrocytes and arterioles during neurovascular coupling. *Circulation Research*, 95, e73–e81.

Gangadhar, G., Joseph, D., & Chakravarthy, V. S. (2007). An oscillatory neuromotor model of handwriting generation. *International Journal on Document Analysis and Recognition, 10*, 69–84.

Gangadhar, G., Joseph, D., & Chakravarthy, V. S. (2008). Understanding Parkinsonian handwriting using a computational model of basal ganglia. *Neural Computation, 20*, 2491–2525.

Gibson, W. G., Farnell, L., & Bennett, M. R. (2007). A computational model relating changes in cerebral blood volume to synaptic activity in neurons. *Neurocomputing, 7*, 1674–1679.

Gonzalez-Lima, F., & Garrosa, M. (1991). Quantitative histochemistry of cytochrome oxidase in rat brain. *Neurosci. Lett., 123*, 251–253.

Goodall, S., Reggia, J. A., Chen, Y., Ruppin, E., & Whitney, C. (1997). A computational model of acute focal cortical lesions. *Stroke, 28*, 101–109.

Haydon, P. G., & Carmignoto, G. (2006). Astrocyte control of synaptic transmission and neurovascular coupling. *Physiol. Rev., 86*, 1009–1031.

Hinton, G. E., Osindero, S., & Teh, Y. W. (2006). A fast learning algorithm for deep belief nets. *Neural Comput., 18*, 1527–1554.

Kager, H., Wadman, W. J., & Somjen, G. G. (2000). Simulated seizures and spreading depression in a neuron model incorporating interstitial space and ion concentrations. *J. Neurophysiol., 84*, 495–512.

Kasischke, K. A., Vishwasrao, H. D., Fisher, P. J., Zipfel, W. R., & Webb, W. W. (2004). Neural activity triggers neuronal oxidative metabolism followed by astrocytic glycolysis. *Science, 305*, 99–103.

Kosko, B. (1992). *Neural networks and fuzzy systems*. Englewood Cliffs, NJ: Prentice Hall.

Lee, T. J. (2000). Nitric oxide and the cerebral vascular function. *J. Biomed. Sci.,* 7, 16–26.

Magistretti, P. J. (2006). Neuron-glia metabolic coupling and plasticity. *Journal of Experimental Biology, 209*, 2301–2311.

Nadkarni, S., & Jung, P. (2003). Spontaneous oscillations of dressed neurons: A new mechanism for epilepsy? *Physical Review Letters, 91*, 268101–268104.

Nadkarni, S., & Jung, P. (2004). Dressed neurons: Modeling neural-glial interactions. *Phys. Biol., 1*, 35–41.

Nadkarni, S., Jung, P., & Levine, H. (2008). Astrocytes optimize the synaptic transmission of information. *PLoS Computational Biology*, 4, e1000088, 1–11.

Nilsson, H., & Aalkjaer, C. (2003). Vasomotion: Mechanisms and physiological importance. *Mol. Interv., 3*, 79–89.

Parri, H. R., Gould, T. M., & Crunelli, V. (2001). Spontaneous astrocytic Ca^{2+} oscillations in situ drive NMDAR-mediated neuronal excitation. *Nat. Neurosci., 4*, 803–812.

Pellerin, L., Pellegri, G., Bittar, P. G., Charnay, Y., Bouras, C., Martin, J. L., et al. (1998). Evidence supporting the existence of an activity-dependent astrocyte-neuron lactate shuttle. *Dev. Neurosci., 20*, 291–299.

Postnov, D. E., Ryazanova, L. S., & Sosnovtseva, O. V. (2007). Functional modeling of neural-glial interaction. *BioSystems, 89*, 84–91.

Pradhan, R. K., & Chakravarthy, V. S. (2007). A computational model that links non-periodic vasomotion to enhanced oxygenation in skeletal muscle. *Math Biosci., 209*, 486–499.

Pradhan, R. K., & Chakravarthy, V. S. (2009). Desynchronized vasomotion and desynchronized fiber activation pattern enhance oxygenation in a model of skeletal muscle. *J. Theor. Biol., 259*, 241–252.

Pradhan, R. K., Chakravarthy, V. S., & Prabhakar, A. (2007). Effect of chaotic vasomotion in skeletal muscle on tissue oxygenation. *Microvasc. Res., 74*, 51–64.

Reggia, J. A., & Montgomery, D. (1996). A computational model of visual hallucinations in migraine. *Comput. Biol. Med., 26*, 133–141.

Revett, K., Ruppin, E., Goodall, S., & Reggia, J. A. (1998). Spreading depression in focal ischemia: A computational study. *J. Cereb. Blood Flow Metab., 18*, 998–1007.

Rose, C. R., & Konnerth, A. (2001). Exciting glial oscillations. *Nat. Neurosc., 4*, 773–774.

Schummers, J., Yu, H., & Sur, M. (2008). Tuned responses of astrocytes and their influence on hemodynamic signals in the visual cortex. *Science, 320*, 1638–1643.

Secomb, T. W., & Pries, A. R. (2002). Information transfer in microvascular networks. *Microcirculation, 9*, 377–387.

Sherwood, C. C., Stimpson, C. D., Raghanti, M. A., Wildman, D. E., Uddin, M., & Rossman, L. I. (2006). Evolution of increased glia-neuron ratios in the human frontal cortex. *Proc. Natl. Acad. Sci. USA, 103*, 13606–13611.

Somjen, G., Kager, H., & Wadman, W. (2008). Computer simulations of neuron-glia interactions mediated by ion flux. *Journal of Computational Neuroscience, 25*, 349–365.

Szeligo, F., & Leblond, C. P. (1977). Response of the three main types of glial cells of cortex and corpus callosum in rats handled during suckling or exposed to enriched, control and impoverished environments following weaning. *J. Comp. Neurol., 172*, 247–263.

Theodosis, D. T., & Poulain, D. A. (1993). Activity-dependent neuronal-glial and synaptic plasticity in the adult mammalian hypothalamus. *Neuroscience, 57*, 501–535.

Tsacopoulos, M., & Magistretti, P. J. (1996). Metabolic coupling between glia and neurons. *J. Neurosci., 16*, 877–885.

Zhang, C., & Wong-Riley, M. (1999). Expression and regulation of NMDA receptor subunit R1 and neuronal nitric oxide synthase in cortical neuronal cultures: Correlation with cytochrome oxidase. *J. Neurocytol., 28*, 525–539

Received January 15, 2009; accepted July 26, 2009.